UKRAINIAN JOURNAL OF MECHANICAL ENGINEERING AND MATERIALS SCIENCE

Vol. 1, No. 1, 2015

Grigorii Beliaiev, Ivan Volosatov, Mykola Kakhovskyi
E.O. Paton Electric Welding Institute, Kyiv, Ukraine

CAUSES OF DUCTILITY-DIP CRACKS FORMATION IN IN52 AND IN52 MSS ALLOYS DURING FUSION WELDING

Received: May 19, 2015 / Revised: August 12, 2015 / Accepted: September 16, 2015

Abstract. The aim of the paper is to investigate one of the causes of ductility-dip cracks (DDC) formation. The main aim of this work is calculation of grain boundaries (GB) cohesive energy in nickel based In52 and In52 MSS alloys. For measuring the GB energy anisotropy methods of thermal etching and light interferometry were used. DDC form on the grain boundaries of nickel based alloys due to adsorption of impurities during multipass welding. The In52 alloy has tendency to form DDC during multipass welding fusion unlike In52 MSS one doped with Mo and Nb. The main cause is the change of thermodynamic state of the GB, as it is indicated by the decrease in the cohesive energy to 1.8-1.26 J/m^2. During multipass fusion welding in In52 alloy adsorption of S and O from the grains body to GB takes place. The average concentration of O and S on the surface of DDC for high angle boundaries is within 2.3-4.5 and 0.5-1 at. %, respectively. Presented in this paper results have shown the influence of welding heat for reduce the cohesive strength of GB and, as a result, of the formation of DDC. Quantitative effect of S and O as embrittlement elements on the value of decrease in the cohesive energy was shown.

Introduction

Formation and crack propagation in polycrystalline metals and alloys occurs at the stage of production, processing or technological operations. The reason for the fall of the strength of metals and alloys is a adsorbtion of impurity atoms at grain boundaries (GBs). Cracking problem is relevant in modern science and technology because of increasing demands for quality and specific strength metallic materials.

Problem formulation

Nuclear electricity rather successfully established itself as a cheap source of electricity. Safety of nuclear reactors in the first place depends from the quality of construction materials and correctness of technological operations during installation and repair. The main structural material of this field of industry is nickel-based alloys. This is due to their high heat resistance and mechanical properties. During work these alloys, as well as when repairing, primarily fusion welding, may sharply increase the propensity to intergranular embrittlement. Plasticity of austenitic high-alloy steels and nickel-based alloys under static tensile tests decreases in the brittle temperature range (BTR) 600-1000˚C. Possible to formation the ductility-dip cracks (DDC) on the GB during the multipass fusion welding. Investigation the fracture surface shows intergranular brittle fracture. Thus occurs abnormally rapid ductile-brittle transition in thin GB areas. Microstructure degradation indicate the probability of occurrence of volumes of metal along the GB, which differs significantly from its initial state.

Analysis of information sources

Crack nucleation and growth in the polycrystalline alloy is characterized by a balance between the kinetics of crack growth and resistance of the alloy [1]. Cohesive energy is a parameter of the resistance of the alloy. This is general characteristics of the bond strength between the grains, which includes the surface energy and GB energy. In case the cohesion energy below a critical level due to the presence of impurity atoms, crack growth resistance decreases. The main factors reducing the cohesive energy can be: the accumulation of dislocations in GB areas, high crystallographic disorientation of neighboring grains, segregation and adsorption of impurity atoms on the GB. Grain boundary adsorption of atoms S, O in

austenitic high alloy leads to the formation the brittle intergranular fracture [2]. The large number of slip systems FCC lattice promotes mass transfer of atoms S, O from body to GB [3]. The authors of [4] studied the effect of sulfur adsorption on the nickel GB and showed that low presence in 5 nm monolayer leads to brittle fracture. Other researchers showed the dependence of disorientation neighboring grains from cohesive energy of fcc metals [5]. In [1] the authors investigated abnormally fast ductile-brittle transition pure polycrystalline nickel at a maximum sulfur content of 50 ppm. The relationship of mechanical properties with cohesive energy GBs metals for different crystal lattices evaluated in [6].

Formulation of goals and tasks of research

This work is based on well-known scientific research data of GB thermodynamic and their own experimental procedures, experiments and calculations of GB energy properties of alloys In 52 and In52 MSS. The aim of the paper is to investigate one of the reason of ductility-dip cracks formation. The main aim this work was calculating grain boundaries cohesive energy in nickel based alloys In52 and In52 MSS.

Experimental procedure and results

It is generally accepted to explain the formation of grooves on etched GB, establishing equilibrium the energies of GB and free surface [7]. The author of [8] observed an abnormal change in the grooves profile of thermal etching in polycrystalline aluminum. There is a direct correlation the purity of the GB from the geometry of the groove etching profile. Similar experiments were carried out by the authors of [9]. Grain boundary energy was compared with the surface energy of the crystal. The surface tension promotes formation groove on the plane of the section in the output place of GB. Under equilibrium conditions, the angles of the groove opening, corresponds to the relative amount of free surface energy and the energy of GB [7].

Figure 1 is a schematic representation of symmetric groove etching. The analysis is reduced to determining the dihedral angle ψ of disclosure grain boundary and $h_{1,2}$ and a, b. Parameters $h_{1,2}$ and a, b determine the degree of plastic deformation in the GB regions. Recent parameters depend on a degree of plastic deformation in GB regions, primarily the density of dislocations [10].

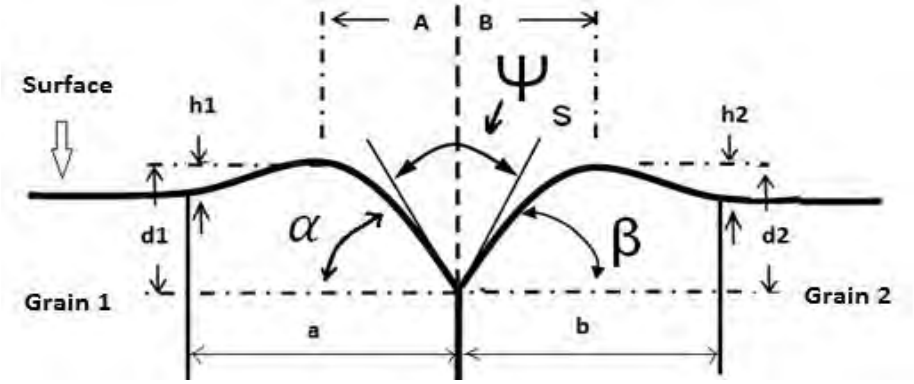

Fig. 1. Schematic representation the etching profile of groove

Generally, the surface energy is isotropic and the etching grooves have a symmetrical shape, the angles α and β are the same. However, many reports indicate a deviation from symmetry [11,12]. The accuracy of the method depends from measurement methodology dihedral angle ψ at the bottom of the groove [13]. In this work, the angle is determined by direct measurement of the cross section, which forms a surface perpendicular to the formation of the etching grooves, given values A, B, d1, d2. The asymmetry of the profile two halves is due to the different surface diffusion coefficient, which depends from the value of the activation energy for diffusion in the GB area. The different crystallographic orientations and the dislocation densities at the GB areas have influence on the activation energy of diffusion. Fig. 2 shows an example the asymmetric profile of etched grooves in alloy FCC after exposure 1400˚C [14].

The width of the GB after etching was measured by direct observation of the profile groove etching. Further, taking into account the geometric features of the etching grooves by formulas (1), (2) was calculated dependence the GB energy E_{GB} to the energy of grain surface E_S. Angles α and β are

calculated separately that take into account asymmetry of the profile, and reduce the measurement error. Width of etching groove W is the sum of the two distances between the etching depth and the maximum height of the profile on both sides W = A + B.

$$\frac{A+B}{d_{1,2}} = \frac{4.73}{tg(a,b)}, \tag{1}$$

$$\frac{E_{gb}}{E_s} = 2\cos\left(\frac{y_s}{2}\right), \tag{2}$$

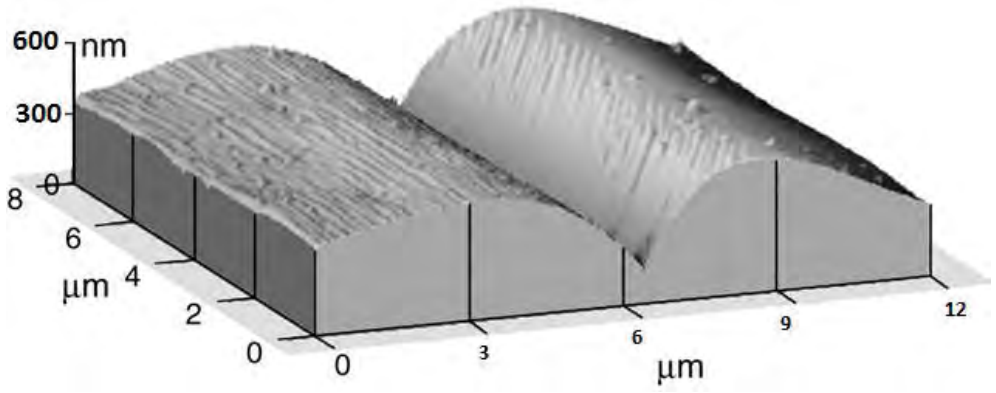

Fig. 2. Profile grooves etched alloy with an fcc lattice [14]

Calculation of the internal energy of GB was performed on the basis of dislocation model proposed by Reid and Shockley. The model takes into account the dependence of GB energy from the orientation of crystal lattice planes in grain and the elastic energy of the dislocation core [15]. They determined that the crystal misorientation compensated by dislocations at the GB. The increase the misorientation angle is proportional to the density of dislocations. The energy of the GB can be expressed mathematically in the form of functional dependence the energy of dislocation core from the misorientation angle of slip planes in the grains.

Accordance with works [16], [17], increasing the contribution of the covalent bond can reduce the cohesive energy and increase susceptibility to embrittlement of GB. One of the reason is adsorption of impurity atoms at grain boundaries or formation dislocation clusters along the interface [18]. The energy of dislocation GB per square centimeter of the surface section ais defining by formulas (3), (4) and (5).

$$E_{gb} = E_0 q\left(A - \ln q\right), \tag{3}$$

$$E_0 = \frac{mb}{4p\left(1-n\right)}, \tag{4}$$

$$A_0 = \frac{4p(1-n)B_k}{mb^2}, \tag{5}$$

m – shear modulus, MPa; b – Burgers vector, nm; n – Poissons ratio; B_k – Energy of the dislocation core, J.

Ductility dip cracking is occurs due the destruction of energy bonds between atoms. Energy E_{gb} «solid» GB is spent on the formation of two new surfaces with energy value E_s. The difference between these two parameters is called cohesive energy E_{coh}, which is a measure of GB strength [19].

$$E_{coh} = 2E_s - E_{gb}, \tag{6}$$

E_{coh} – cohesive energy, J/m^2; E_s – surface energy, J/m^2; E_{gb} – grain boundary energy, J/m^2.

Embrittling elements reduce the surface energy E_s greater than the energy of GB E_{gb}. Changing the type of atomic bonding at GB due adsorption can reduces the cohesive energy E_{coh}. In calculating the value of adsorption energy of impurity on the grain surface is negative. Enthalpy of each impurity and density of

atoms A (atoms / m^2), in formula (7) allow to calculate the cohesive energy of the grain boundaries after adsorption:

$$E_{coh} = 2E_s - E_{gb} - \left(\Delta E_{gb}^{ad} - \Delta E_s^{ad}\right) \cdot A, \quad (7)$$

$\left(2E_s - E_{gb}\right)$ – cohesive energy after adsorption, J; ΔE_{gb}^{ad} – enthalpy of impurities adsorption on the Gb, J; ΔE_s^{ad} – enthalpy of impurities adsorption on the surface of grains, J; $\left(\Delta E_{gb}^{ad} - \Delta E_s^{ad}\right)$ – energy contribution of adsorption, J; A - density of impurities, nm^{-1}.

For investigation were selected nickel superalloys In52 and In52 MSS in the initial state and after fusion welding. Alloy In52 MSS has a high resistance to form DDC due alloying by Nb and Mo. Chemical composition of the alloys is shown in Table 1, 2.

Table 1

Eigen-frequencies of a clamped-free uniform isotropic beam obtained by means of FEM

Concentration of element, mass %											
C	Mn	Ni	Cr	Fe	Nb+Ta	Mo	Ti	S	P	Al	Si
0.021	0.24	59.17	29.19	9.99	<0.01	0.01	0.51	0.001	0.003	0.72	0.12

Table 2

Eigen-frequencies of a clamped-free uniform isotropic beam obtained by means of FEM

Concentration of element, mass %											
C	Mn	Ni	Cr	Fe	Nb	Mo	Ti	S	P	Al	Si
0.024	0.29	54.55	30.3	8.24	2.52	3.45	0.25	0.002	0.0055	0.22	0.15

The work was performed on a scanning electron microscope Quanta 200 3D with a secondary electron detector Everhart-Thornley (EBSD) and heating table. Observations focused on high-angle GB, as the main places of formation DDC [20]. Measurement the geometric dimensions of the GB profile was performed on the light microinterferometer Linnika MII-4. Images of the sample surface with interference lines held by camera Tucsen Camera 5.0 for metallographic studies. Profiles of the groove etching were measured via software ImageJ, pre-calibrated for interferometer. Marks were placed by microhardness tester Shimadzu.

Two samples were cut with proportions: 5 mm in diameter and 3.2 mm in height. The materials of samples are remelt ingot of wire alloy In52 and In52 MSS in a state before welding fusion. After preparing the surface of samples with using hardness tester Shimadzu M on some places were applied markers on the grains for subsequent studies labeled region. Prior to placing the samples in a microscope chamber was made careful polishing the surface by colloidal silica solution Eposil F with a particle size of 0.1 microns.

For investigate GB with DDC samples were cut from a multipass weld in a place of formation microcracks in dissimilar multipass welding. Welding is carried out on an alloy In690 by wires In52 and In52 MSS. Selection the place of investigation and preparation the samples were carried out in the same manner as for the samples in the initial state.

The first part of the study was determination the crystallographic orientation of grains in the tagged region.

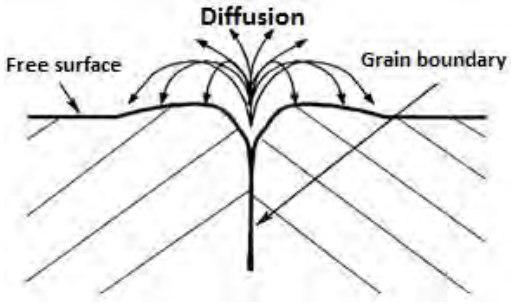

Fig. 3. Schematic representation the kinetics of diffusion atoms

After determining the crystallographic orientation in samples their surfaces were etched in the vacuum chamber of the microscope. Fig. 4 showed SEM table for heating. The maximum heating temperature is 1300˚C, sample heating rate is 50 ° C / min. Exposure time is 3 hours. For improving image quality during etching was used filter (Heat Shield Bras) with supply voltage 22-300 V. Filter changes the speed of the electrons emitted from the heated sample to the initial value at room temperature. With increasing temperature, the sample surface is cleared from oxygen and other surface contaminants. The kinetics of this process determines the thermodynamic state of the GB. Fig. 3 shows a schematic representation of surface atoms diffusion.

Fig. 4. SEM heating table

To reduce the errors in the measurement the each GB was analyzed in 6-8 different places.

The calculation of the real height and depth in etched GB was evaluated by the formula (9) for the green filter [21]:

$$d,h = \frac{0.5\,l\,\Delta N}{k}, \tag{9}$$

λ – wave length for green filter, λ = 0,55 μm; ΔN – height of the band bending, μm; k – interval between the interference lines, μm.

Investigation the microstructure of alloys In52 and In52 MSS was performed within 4-6 grains. Image of marks and electronic image crystallographic orientation for the two alloys in state before fusion welding is shown in Fig. 4 b and 5 b, respectively. For further identify the grains were numbered.

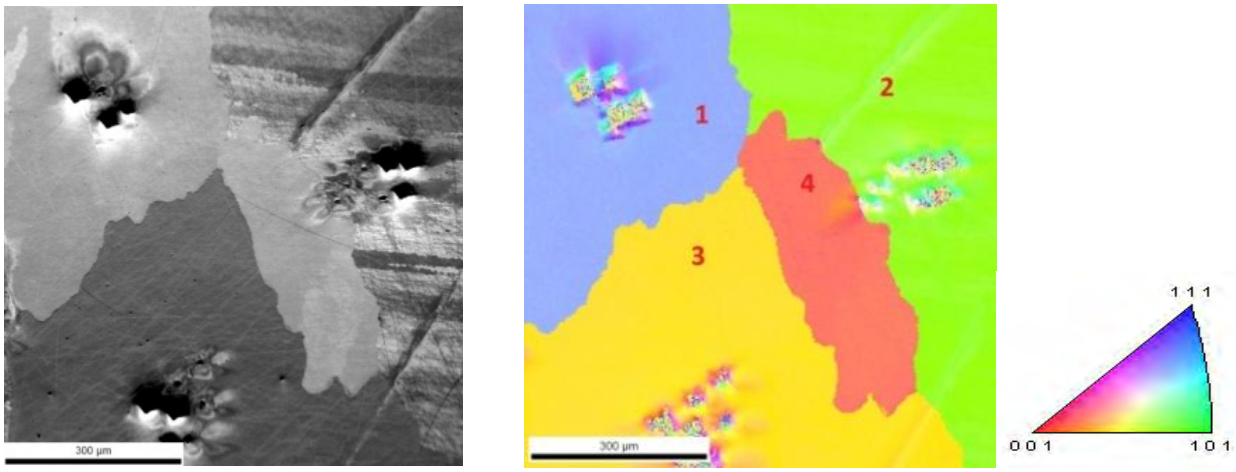

a) *b)*

Fig. 4. a - SEM image of marks on GB alloy In52;
b – EBSD map of crystallo-graphic orientation the grains of alloy In52

According to SEM data the total length of GB in the field of view with marks are 1.09 cm and 1.04 cm for In52 and In52MSS alloys, respectively. This is mainly the high angle grain boundaries with angles of misorientation within 30-60˚.

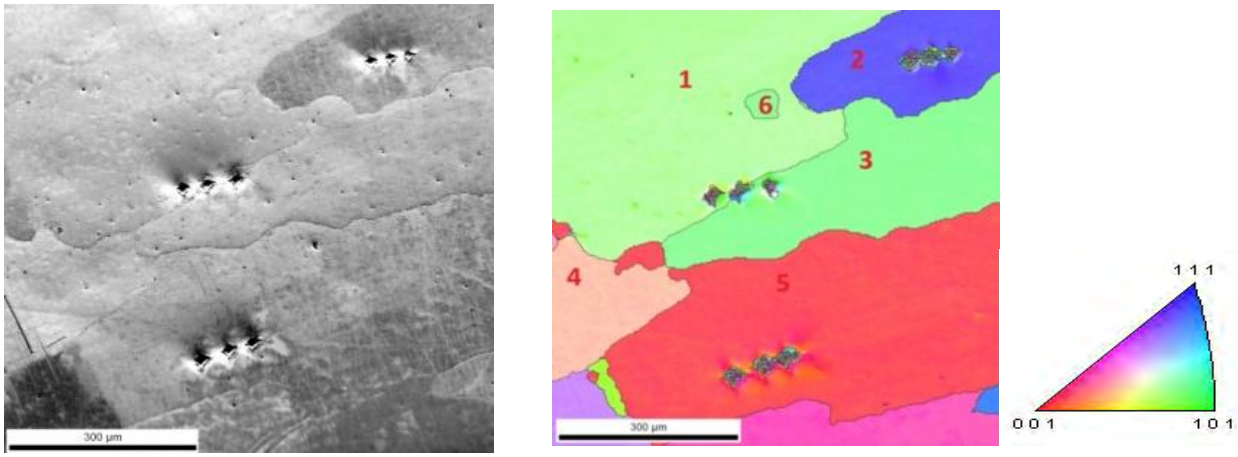

a) *b)*

Fig. 5. a – SEM image of marks on GB alloy In52 MSS;
b – EBSD map of crystallographic orientation the grains of alloy In52 MSS

Visual observation of etching process in two alloys showed that they are quite sensitive to the temperature rise. When the temperature reached to 900˚C begins the process of thermal etching on the GB. For example, the beginning of etching the commercially pure nickel is in the temperature range of 1200-1300˚C. This is explained by a lower activation energy for surface diffusion of atoms due presence S, O on GB or accumulation of dislocations. Images of GB condition in alloys during etching under 900-1000˚C are shown in Fig. 6 a, b.

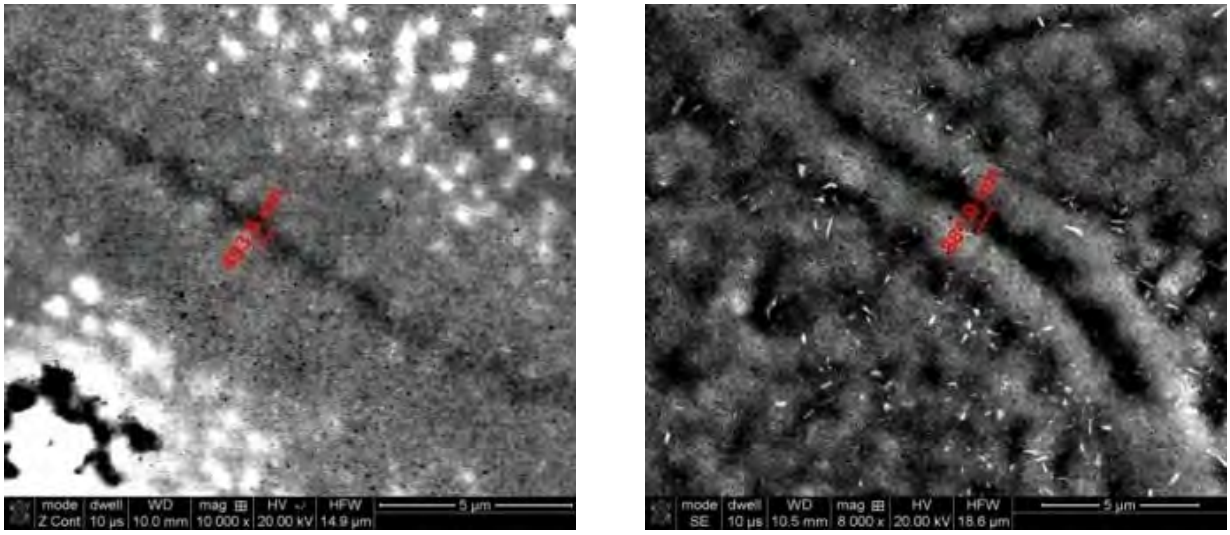

a) *b)*

Fig. 6. a – SEM image of marks on GB alloy In52 MSS;
b – EBSD map of crystallographic orientation the grains of alloy In52 MSS

After that, etched surfaces were studied on the light interferometer. For reducing measurement errors were calculated 4-8 light lines for each GB profile. Fig. 7 a, b shows an image of the interference lines on GB for two alloys. The total amount of measurements is 80 light lines. For a visual representation of geometric shapes GBs on calculated data, made for formula 1,2,6, were built schematic profiles GBs with different crystallographic misorientation, Fig. 8 a, b.

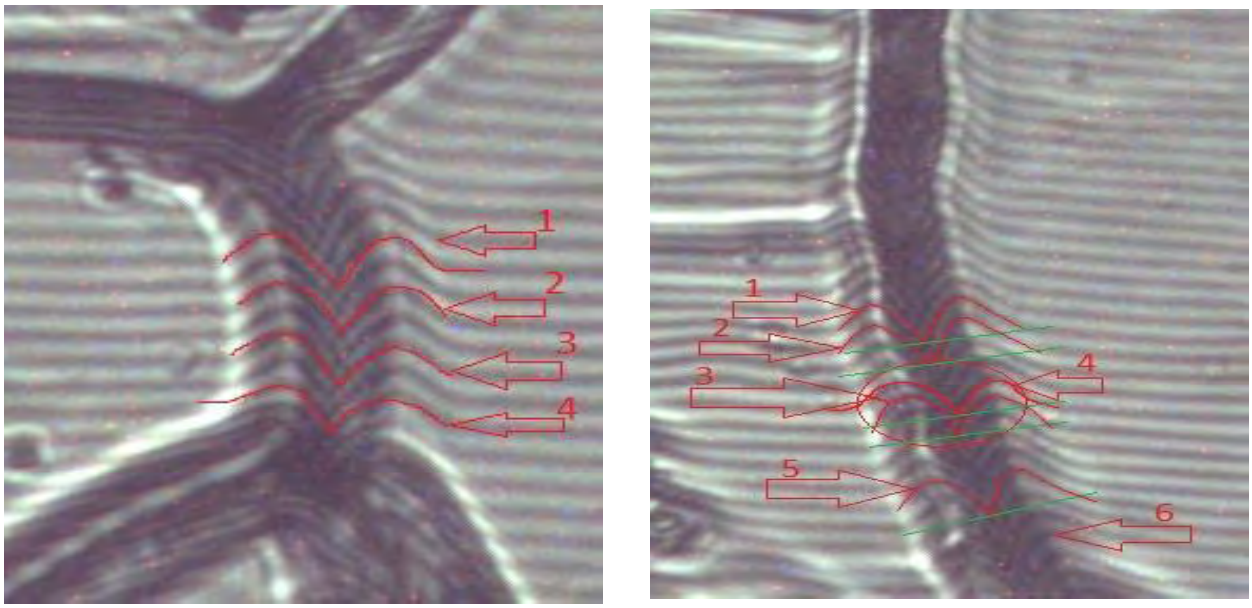

a) *b)*

Fig. 7. a – interference lines of GB 1–4 alloy In52; b – interference lines of GB 1–4 alloy In52 MSS

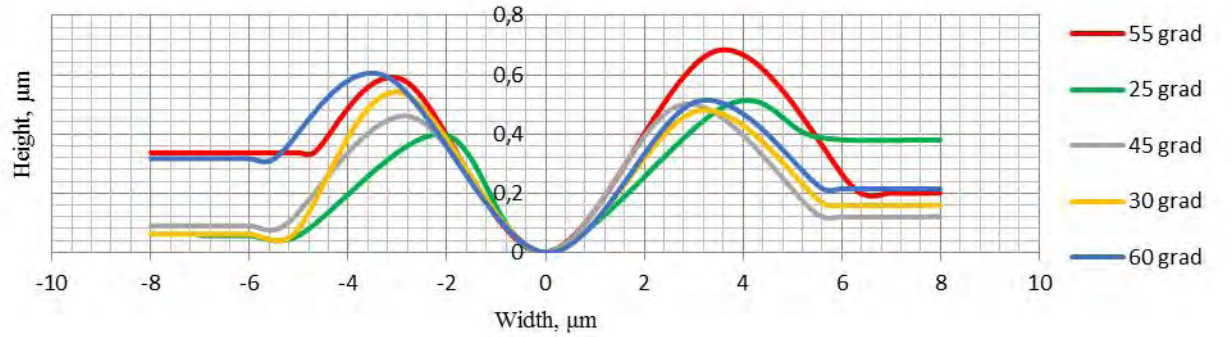

a)

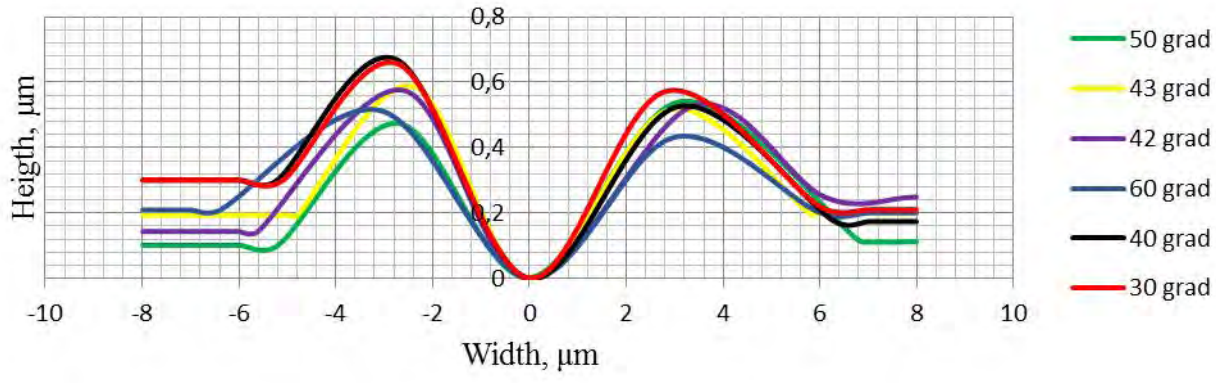

b)

Fig. 8. a – schematic profile of the GB, alloy In52; b – schematic profile of the GB, alloy In52 MSS

According to Griffith`s model of destruction, considering the formulas 1-5, were calculated the energy parameters of GB,which depending from crystallographic misorientation grains in the alloy. The values of energies for GB, surface, cohesion and width of GB for two alloys in a state before welding are shown in Table 3. The last column indicates the number of GBs from Fig. 4 b and 5 b.

Table 3

Grain boundaries parameters

Alloy	Θ, grad	γ_{gb}, J/m^2	γ_{coh}, J/m^2	γ_S, J/m^2	W, μm	Ψ, grad	№ GB
In 52	25	0,77	4	2,42	5,9	163	3-4
	30	0,78	3,8	2,3	6,2	162	1-4
	45	0,68	3,33	2	5,6	161	4-2
	55	0,55	2,33	1,44	6,4	158	1-3
	60	0,46	2,12	1,27	6,4	160	1-2
In 52 MSS	30	0,78	2,76	1,71	5,6	155	3-5
	40	0,69	2,78	1,73	5,9	157	2-3
	42	0,71	2,95	1,85	6,4	157	1-2
	43	0,71	2,77	1,74	6,0	156	1-4
	50	0,62	2,64	1,63	5,9	159	1-3
	60	0,46	2,5	1,48	6,1	163	1-6

During multipass fusion welding possibly the cracks formation on the GB in alloy In52. The thermodynamic state of GB in alloy In52 MSS is without significant changes after welding. Ductility dip cracks are not observed and the energy values correspond to the units for initial state.

The crystallographic orientations of the grains in alloy In52 with DDC on high-angle GB after fusion welding are shown in Fig. 9. Cracks are formed on the GB with the crystallographic misorientation within 45-60˚. Such high angle boundaries in the initial state have a decreased cohesive energy inside of 3,33-2,12 J/m^2. Welding heat creates tension in the body of grains, which lead to generation a new dislocation sources and accumulation dislocations along the GB. Abnormal mass transfer of impurity atoms from the body to GB decreases the cohesive energy until 1-2 J/m2 due adsorption of S and O.

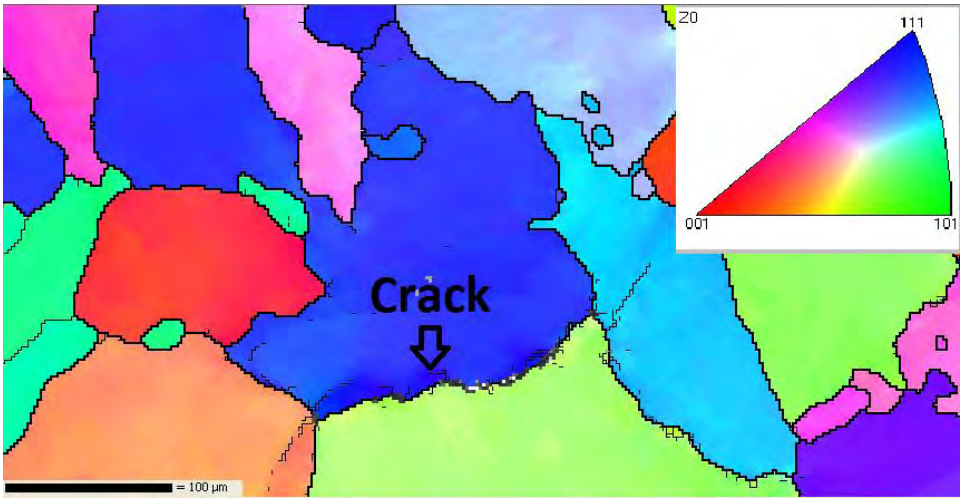

Fig. 9. Crystallographic orientation grains at the place of DDC, alloy In 52

Farther on the microinterferometer were analyzed 3 GB with DDC in the range of misorientation angles witjin 45-60˚ and 17 GB without cracks. The number of measured interference lines was more than 100. The main places of investigation were outfalls. The thermodynamic parameters of GBs state with DDC are listed in Table 4.

Table 4

Grain boundaries parameters

	Θ, grad	γ_{gb}, J/m^2	γ_{coh}, J/m^2	γ_S, J/m^2	W, μm	Ψ, grad	№ GB
In 52	45-60	0,46	1,8	1,15	6,6	157	1
		0,55	1,31	0,93	6,7	146	2
		0,68	1,26	0,97	6,6	139	3

Some GB has breaks (interferometer lines are cut off). The phenomenon can be explained by the theory of abnormally rapid mass transfer of impurities along the slip bands. The cohesive energy along GB is discrete. This process depended from dislocation density and purity in the GB areas.

Fig. 10 shows a dependence of cohesive energy from grains misorientation angle in the initial state and after fusion welding in alloy In52. The curve indicates that the GB microstructure degradation occurs over a range of angles 45-60˚. Reducing the cohesive energy GBs on misorientation angles 55-60˚ is 1.1-1.3 J / m^2. This is sufficient to reduce the tensile strength on the level of local stresses which are generating during cooling after fusion welding [22]. For formula 7, taking into account the energy of adsorption the chemical elements on the GBs surface can estimate the concentration of impurities which provide DDC. Among all possible embrittling elements in the alloy the most harmful are sulfur and oxygen. Oxygen diffuses into the molten metal from the atmosphere during fusion welding. The maximum solubility of oxygen in the weld metal according to the phase diagram is 0.0045 wt. % [23]. Mass transfer of oxygen from the grain body to GB is performed in the process of heating and cooling during the next welding pass. Oxygen formed on the grain surface an adsorption layer of a few nanometers in width. Table 5 shows the calculated values of S and O enthalpy for commercially pure nickel [24] as a basis alloy In52. According to the work, the center of crystal face is the most likely placement for sulfur atoms in the fcc nickel lattice. Ni-3d and S-3p hybridization play an important role in the formation of electronic communications. If alloy is doped a large amount of chromium can be increasing the enthalpy [25].The distance between nickel atoms and impurities, taking into account the geometry of the atoms location in the crystal lattice and the lattice period, allows us to calculate the density of nickel atoms and impurities per 1 m^2.

Table 5

Grain boundaries parameters

Impurity	Adsorption site	Ni (111)	
		ΔE_{gb}^{ad} (eV/atom)	d , $\dot{A}$
S	Center	-4.99	2.15
	Top	-3.55	2.02
	Interstitial	-4.74	2.10
O	Center	-5.56	1.85
	Top	-3.87	1.84
	Interstitial	-5.28	1.84

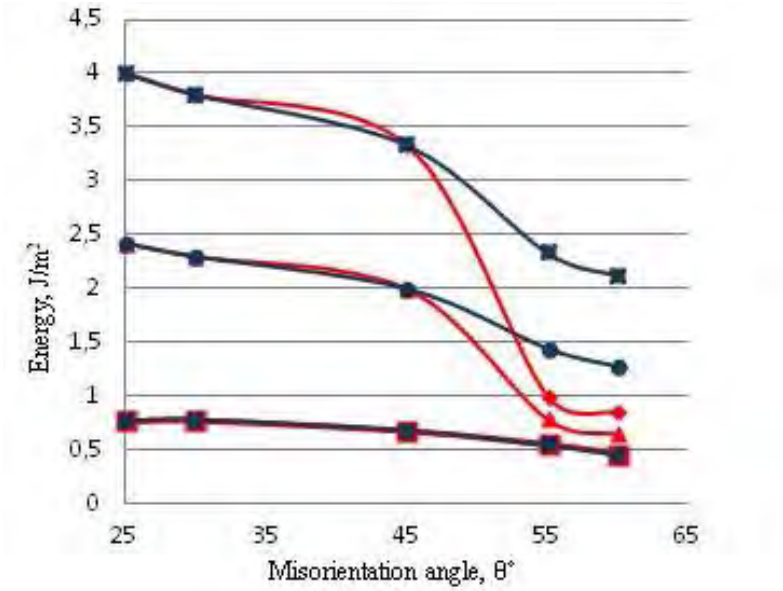

Fig. 10. The dependence of cohesive energy E_{coh} from misorientation angle θ in alloy In52

Table 6 shows the maximum concentration of S and O (in at.%) that reduce the cohesive energy to a value of DDC formation, considering the fact that elements are separated. If we consider the maximum bulk solubility of oxygen in the liquid nickel and initial bulk concentration of sulfur in the alloy, the proportional relation between them is 4.5-5 times. Thus, given similar adsorption energy of O and S on the GB, it can be assumed that the GB concentration of oxygen is 4.5-5 times higher than sulfur. Table 6 shows the calculated data of concentration which was measured directly on the surface of DDC, Ccrack(S) and Ccrack(O).

Table 6

Dependence of S and O concentration from cohesive energy Ecoh (calculated)

Misorientation angle, θ, grad	Ecoh, J/m^2	C_{max}, at.% S	C_{max},at. % O	C_{crack}, at.% S	C_{crack}, at.% O
45	3,80	0	0	0	0
	3,5	1	0,8	0,16	0,7
	3	2,40	2,2	0,40	1,8
	2,5	3,9	3,5	0,67	2,9
	2	5	4,8	0,9	4
	1,8	6	5,4	1	4,5
55	3,33	0	0	0	0
	3	0,95	0,85	0,16	0,7
	2,5	2,45	2,2	0,4	1,8
	2	3,9	3,5	0,67	2,9
	1,5	5,4	4,8	0,9	4
	1,31	6	5,4	1	4,4
60	2,33	0	0	0	0
	2	0,98	0,88	0,16	0,73
	1,8	1,60	1,44	0,27	1,2
	1,65	2	1,8	0,34	1,5
	1,5	2,47	2,2	0,42	1,8
	1,26	3,2	2,88	0,5	2,3

The data of Table 6 are shown in Fig. 11 for high-angle GB in the angular range 45-60˚. Due to the higher solubility of oxygen in the weld metal, its influence as embrittling element carries more weight. The accuracy of the theoretical calculations confirmed by direct observations of concentration S and O on the surface of open DDC in the chamber of Auger spectrometer. Purification the surface of DDC from impurities which was absorbed from the atmosphere after the break, was performed by ion etching. Etching speed is10 nm/min. Concentration curves of S and O coincides on the entire range of etching, which is explained almost equal energy adsorption ΔE_s^{ad} .

The difference between points on the curves is 4.5-5 times that confirms the assumption of same enthalpy value which described above. Thus, the average concentration of O and S on the surface of DDC for high angle boundaries is inside of 2,3-4,5 and 0.5-1 at. %, respectively (Fig. 12).

Conclusions

Complex of research, which includes scanning electron microscopy with heating, light micro interferometry, and Auger spectral analysis were described in this work. We obtained the following micro structural and thermodynamic parameters of In52 and In52 MSS alloys: disorientation angle of neighboring grains, surface, grain boundaries, and cohesion energies, S and O concentrations on the surface of DDC.

1. It was found that the cohesive energy E_{coh} of GB depends on misorientation angle θ in neighboring grains. With the increase in misorientation angle θ, the cohesive energy decreases. Less resistant to formation of DDC are high-angle grain boundaries with the range of misorientation within 45-60°. Average E_{coh} are 3.1 and 2.9 J/m^2 for In52 and In52 MSS alloys, respectively.

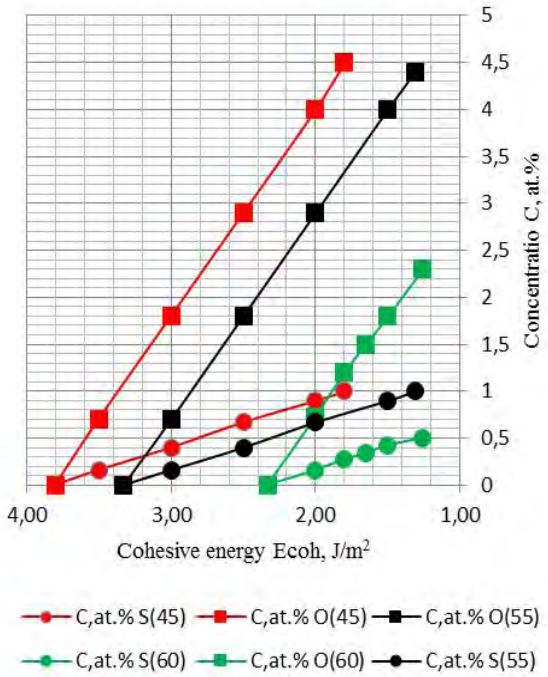

Fig. 11. Dependence of S and O concentration from cohesive energy Ecoh (calculated)

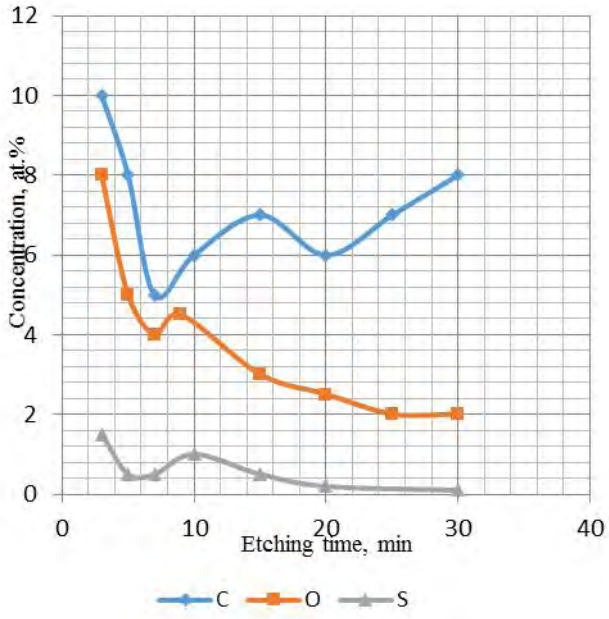

Fig. 12. Experimental concentration of impurities on the surface of DDC

2. The In52 alloy has tendency to form DDC during multipass welding fusion. The main cause is the change of thermodynamic state of the GB, it is indicated by the decrease in the cohesive energy to 1.8-1.26 J/m^2. Cracks form in the high-angle GB within 45-60°, that in the initial state have lower cohesive energy.

3. One of the causes of the cohesive energy decrease in In52 alloys during multipass fusion welding is adsorption of S and O from the grains body to GB. The adsorption on the GB is performed due to abnormally rapid mass transfer of impurities during heating and cooling the welded metal in the time of the next welding pass.

4. The maximum bulk solubility of oxygen in the liquid weld metal is 4.5-5 times larger than the original volume concentration of sulfur in the alloy. Given similar energy absorption S and O on the GB, it can be assumed that GB concentration of oxygen is 4.5-5 times higher than that of sulfur.

5. The concentration curves of S and O coincide on the entire range of etching, which is explained by almost equal energy adsorption ΔE_{gb}^{ad}. The difference between points on the curves is 4.5-5 times larger that confirms the assumption of same enthalpy value. The average concentration of O and S on the surface of DDC for high angle boundaries is within 2.3-4.5 and 0.5-1 at. %, respectively.

References

[1] S. Mahalingam, P.E.J. Flewitt, J.F. Knott: The ductile–brittle transition for nominally pure polycrystalline nickel, Materials Science & Engineering A 564 (2013) 342–350.

[2] Alan F.Lin, Mechanics and Mechanism of fracture, ASM International, 2005, pp. 458.

[3] Lahtin Ju.M. Metallovedenie i termicheskaja obrabotka metallov. – M. : Mashinostroenie, 1983. – 359 p.

[4] D.H. Lassila, H.K. Birnbaum, Acta Metall. Mater. 35 (1987) 1815–1822.

[5] Elizabeth A. Holm, David L. Olmsted and Stephen M. Foiles, Scripta Materialia, Comparing grain boundary energies in face-centered cubic metals: Al, Au, Cu and Ni 63 (2010) 905–908.

[6] Kazuhisa Miyoshi, Donald H. Buckley, Relationship between the ideal tensile strength and the friction properties of metals in contact with nonmeatls and themselve, NASA Technical Paper 1883 (1981).

[7] B. Chalmers, R. King, R. Shuttleworth, Proc. Roy. Soc., 1948, A193, 465.

[8] Woosuck Shin, Won-Seon Seo, Kunihito Koumoto, Grain-boundary grooves and surface diffusion in polycrystalline alumina measured by atomic force microscope Journal of the European Ceramic Society 18 (1998) 595-600.

[9] Woosuck Shin, Won-Seon Seo, Kunihito Koumoto, Grain-boundary grooves and surface diffusion in polycrystalline alumina measured by atomic force microscope, Journal of the European Ceramic Society 18 (1998) 595-600.

[10] Jennifer L.W. Carter, Michael W. Kuper, Michael D. Uchic, Michael J. Mills, Characterization of localized deformation near grain boundaries of superalloy Rene-104 at elevated temperature, Materials Science & Engineering A 605 (2014) 127–136.

[11] Gregory S. Rohrer Grain boundary energy anisotropy: a review J Mater Sci (2011) 46:5881–5895.

[12] E. Rabkin, L. Klinger, V. Semenov, Grain boundary grooving at the singular surfaces, Acta mater. 48 (2000) 1533-1540.

[13] H. Gleiter, B. Chalmers, High-angle grain boundaries (progress in materials science, Vol. 16). (1972). 274 Seit., zahlreiche Abbild. und Tab. — Pergamon Press, Oxford, New York, Toronto, Sydney, Braunschweig, 1972.

[14] D. San Martin, Y. Palizdar, R.C. Cochrane, R. Brydson, A.J. Scott, Application of Nomarski differential interference contrast microscopy to highlight the prior austenite grain boundaries revealed by thermal etching, Materials characterization 61(2010), pp. 584–588.

[15] H.G. Van Bueren, Imperfections in Crystals. North-Holland, Amsterdam; Interscience, New York, 1960. 676 pp.

[16] Mastake Yamaguchi, First-principles study on the grain boundary embrittlement of metals by solute segregation: Part I. Iron (Fe)-Solute (B, C, P, and S) systems, Metallurgical and materials transactions, vol. 42A, February 2011. – 319.

[17] Yokobori T., Otsuka A., Takahashi T., Fracture of Solids, Drucker D.C., Gilman J.J. Ed., AIME, Interscience, 1963, p.261.

[18] P.E.J. Flewitt, R.K. Wild, Grain Boundaries, their Microstructure and Chem-istry, John Wiley & Sons Ltd, Chichester, 2001.

[19] J.R. Rice and J.-S. Wang : Mater. Sci. Eng., 1989, vol. A107, pp. 23–40.

[20] Y. Cheng, Z.H. Jin, Y.W. Zhang, H. Gao, On intrinsic brittleness and ductility of intergranular fracture along symmetrical tilt grain boundaries in copper, Acta Materialia 58 (2010) 2293-2299.

[21] V. I. Kabanova, 3. A. Kulikova, A. N. Peshhenko, D. F. Kitaev Recenzenty: A. I. Bekrenev, Je. D. Posypajko, Interferencija sveta, Kujbyshevskij ordena Trudovogo Krasnogo Znameni aviacionnyj institut im. akademika S. P. Koroleva, metodichka, 1985 g, 16 str.

[22] Abdul Ghani, Residual stresses and heat treatments for metallic welded components, Dublin City University School of Mechanical and Manufacturing Engineering, 1994, pp. 265.

[23] H. Okamoto Ni-O fournal of Phase Equilibria and diffusion august 2007, Vol. 28, Issue 4, p. 408.

[24] Oleksandr I. Malyia, Zhong Chena, Vadym V. Kulisha, Kewu Baib, Ping Wuc, Density functional theory study of the effects of alloying additions on sulfur adsorption on nickel surfaces, Applied Surface Science 264 (2013) 320–328.

[25] Nishith Kumar Das, Tetsuo Shoji, A density functional study of atomic oxygen and water molecule adsorption on Ni(1 1 1) and chromium-substituted Ni(1 1 1) surfaces, Applied Surface Science 258 (2011) 442– 447.